Segment-Weighted Information-Based Event-Triggered Mechanism for Networked Control Systems

Zhou Gu, *Member, IEEE*, Dong Yue, *Fellow, IEEE*, Choon Ki Ahn, *Senior Member, IEEE*, Shen Yan, and Xiangpeng Xie, *Member, IEEE*

***Abstract*—In this study, the event-triggered problem of networked control systems (NCSs) is investigated, and a novel information transmission scheme is established. Under this scheme, the segment-weighted information (SWI) in a sliding historical window (SHW) is calculated and then sampled. Compared with the traditional direct sampling method, in this approach, the control input includes historical information in the SHW, thereby leading to less information loss due to sampling. This study also emphasizes on designing an SWI-based event-triggered mechanism (ETM) for scheduling network transmission. Different from most of the existing ETMs, the proposed SWI-based ETM leverages historical information to determine which data are necessary for the whole control system. Our approach can greatly reduce the number of unexpected triggering events of a control system with stochastic disturbances owing to the introduction of the SWI in the ETM. Moreover, Zeno phenomena are prevented thanks to periodic sampling. Sufficient conditions are derived based on the Lyapunov functional approach, and a numerical simulation example is provided to demonstrate the effectiveness of the proposed method.**

***Index Terms*—Event-triggered mechanism (ETM), networked control system (NCS), segment-weighted information (SWI), sliding historical window (SHW).**

I. Introduction

OWING to the rapid development and ever-increasing application of communication technologies, more and more control systems are being equipped with a network for signal transmission. During the last two decades, networked control systems (NCSs) have attracted growing interest [1], [2], [3], [4]; the information is shared among the sensors, controllers, and actuators through a communication network. Owing to the limited network bandwidth, engineers encounter certain challenges when modeling and analyzing NCSs; some examples are network congestion [5], [6], [7], [8], networked-induced delay, packet dropout and disordering during transmission [9], [10], and constraints regarding the energy, communication, and computational resources.

Sampling and release are essential actions of NCSs. Reseaches have extensively investigated sampled-data control for continuous-time systems with sampled-data outputs. In general, there are two relatively mature sampled-data control methods. The first method is the periodic sampling scheme. Most of the published research results and applications are based on this scheme. The focus of these studies was to determine approaches that ensure stability and stabilize a system with a lower level of conservatism. For example, in [11], the stability of sampled-data control systems with uncertainty is assessed with a Lyapunov–Krasovskii functional method. The researches in [12] constructed time-dependent Lyapunov functionals to obtain the upper bound of the sampling period. To establish a time-dependent Lyapunov functional method with a lower level of conservatism, the researches in [13] created a stabilization approach based on Wirtinger's inequality. In this time-triggered mechanism (TTM), the worst situation in which the system works is usually considered for the selection of a fixed sampling period. Therefore, hardware costs and the consumption of communication and computational resources increase inevitably. Consequently, the second type of sampling scheme (i.e., aperiodic sampling) has gained much attention. The main problem of this scheme is estimating the maximum sampling interval to ensure that the system remains stable [14]. Transforming a system into a time-delay system [15], hybrid system [16], and discrete-time system [17] is a popular way to analyze a system with an aperiodic sampling scheme.

As previously mentioned, periodic sampling and release may result in the waste of network and computational resources. The study of the event-triggered mechanism (ETM) has become a hot topic to alleviate the network burden. In the ETM, the choice to release or sample depends on an event-triggered condition instead of a predetermined fixed period.

Manuscript received 20 April 2022; revised 1 August 2022 and 22 September 2022; accepted 12 October 2022. Date of publication 27 October 2022; date of current version 20 July 2023. This work was supported in part by the National Natural Science Foundation of China under Grant 62273183, Grant 62022044, and Grant 62103193, and in part by the National Research Foundation of Korea (NRF) Grant funded by the Korea Government (Ministry of Science and ICT) under Grant NRF-2020R1A2C1005449. This article was recommended by Associate Editor R.-E. Precup. *(Corresponding authors: Choon Ki Ahn; Dong Yue.)*

Zhou Gu and Shen Yan are with the College of Mechanical and Electronic Engineering, Nanjing Forestry University, Nanjing 210037, China (e-mail: gzh1808@163.com; yanshenzdh@gmail.com).

Dong Yue and Xiangpeng Xie are with the Institute of Advanced Technology, Nanjing University of Posts and Telecommunications, Nanjing 210023, China (e-mail: medongy@vip.163.com; xiexiangpeng1953@163.com).

Choon Ki Ahn is with the School of Electrical Engineering, Korea University, Seoul 136-701, South Korea (e-mail: hironaka@korea.ac.kr).

Color versions of one or more figures in this article are available at https://doi.org/10.1109/TCYB.2022.3215015.

Digital Object Identifier 10.1109/TCYB.2022.3215015

The ETM determines the next sampling instant and the next release instant. For example, Girard [18] and Ge et al. [19] created a dynamic ETM by introducing dynamic variables to determine the next sampling instant. These types of ETMs essentially involve the aperiodic sampling scheme. The Zeno phenomenon is a challenging issue that should be considered in the study of ETM design. To solve this problem, discrete event-triggered strategies (DETSs) [20], [21], [22] for linear networked systems were investigated to decrease the data transmission rate and save network bandwidth. Wen et al. [23] combined the DETS and sliding-mode control method to design a control strategy for nonlinear systems. The DETS uses a TTM for sampling and an ETM for release; the Zeno phenomenon can be easily excluded by physical means. Extended DETSs are widely applied in NCSs. For example, the threshold of the ETM in [7] was designed as an adaptive variable; hence, the data-release rate is adjusted with the state variation. Hu et al. [24] and Gu et al. [25] developed a resilient event-triggered transmission protocol that addresses denial of service (DoS) attacks. In [26], similar transmission scheme was developed for semi-Markovian switching cyber-physical systems. Based on the past transmitted information, a class of memory-based ETMs was investigated in [27] and [28]. However, under this type of ETM, only a few discrete packets can be used to improve the triggering mechanism. Selivanov and Fridman [29] investigated a trade-off event-triggered method between a DETS and continuous ETM by using a switched system approach, under which the ETM is executed after a fixed waiting time to prevent the Zeno phenomenon. Although this method uses a continuous-time state as the ETM input, a waiting period is needed to prevent the Zeno phenomena. A controller with general sampling methods loses vital information of the plant during the fixed sampling period; however, few researches have focused on this problem; therefore, it is one of the main motivations of this study.

Historical information is essential for both the controller and ETM to ensure a good control performance and data-release rate [30], [31]. In practical systems using traditional ETMs, information at a certain instant may trigger unexpected packets. Thus, the burden on the network bandwidth increases, in particular, when the system is subject to random disturbances. A continuous-type ETM (e.g., integral-type ETM) can introduce historical information into the system [32], [33]. However, it is difficult to ensure the interevent time. In addition, a system with a memory-based control strategy can achieve a better control performance than one with a memoryless control strategy. However, few researches have considered these challenging problems of event-triggered control systems.

This study focuses on the design of a new SWI-based event-triggered control strategy for NCSs. The main contributions of this study are highlighted as follows.

1) A novel event-triggered control strategy for NCSs that combines the advantages of the DETS and continuous ETM is presented. Unlike in the conventional periodically sampled event-triggered system, an SWI module is introduced before sampling. The input of the designed ETM uses the segment-weighted information (SWI) in a sliding historical window (SHW) to determine the next event-triggering instant. It can significantly reduce the amount of unexpected released data compared to the already existing communication mechanisms, in particular, for a system with uncertain stochastic disturbances.
2) The SWI in an SHW is split into N segments. The closer information to the current instant, the greater the weight of the SWI is. Our approach has a better control performance than traditional memoryless control strategies because the control input introduces sampled SWI with historical information.

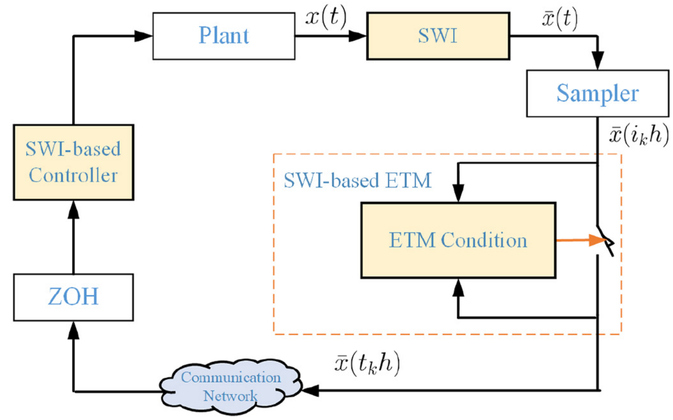

Fig. 1. Framework of SWI-based event-triggered control method.

Notation: Let $\mathbf{He}(X) := X^T + X$ and $\mathbf{Sy}(M, N) := N^T M N$; I_r is the $r \times r$ identity matrix and $\mathbb{I}_j := [\underbrace{0, \ldots, 0}_{j-1}, I, 0, \ldots, 0]$.

II. Preliminaries and Problem Formulation

The physical system is described by the following continuous-time linear system:

$$\begin{cases} \dot{x}(t) = Ax(t) + Bu(t) + Ed(t) \\ z(t) = Cx(t) \end{cases} \tag{1}$$

where A, B, C, and E are known real matrices of appropriate dimensions, $x(t) \in \mathbb{R}^n$ is the state vector; $u(t) \in \mathbb{R}^m$ is the control input; $z(t) \in \mathbb{R}^r$ is the output; and $d(t)$ is an exogenous disturbance belonging to $\mathscr{L}_2[0, \infty)$.

To exploit the historical information in the control loop, a new variable with SWI from $t - w$ to t is introduced

$$\bar{x}(t) = \sum_{p=1}^{N} \frac{\mu_p}{\bar{w}} \int_{t-w_p}^{t-w_{p-1}} x(s)ds \tag{2}$$

with $w_0 = 0$, $w_N = w$, where $\sum_{p=1}^{N} \mu_p = 1$ and $\cup_{i=1}^{N}[t - w_{p-1}, t - w_p) = [t - w, t)$; $t - w$ to t represents the SHW.

For a convenient design, setting $w_p - w_{p-1} = \bar{w}$ yields $w_p = p\bar{w}$, where $\bar{w}$ is a known constant.

As is shown in Fig. 1, the SWI is sampled periodically with the sampling period h and transmitted over the network at instant $t_k h$ only when it satisfies the prescribed triggering condition where $0 < t_0 < t_1 \cdots < t_k \cdots$. The zero-order hold (ZOH) is needed before the signal from the network enters the controller. Subsequently, a quasi-state feedback control strategy is constructed

$$u(t) = K\bar{x}(t_k h) \tag{3}$$

for $t \in [t_k, t_{k+1})$.

Remark 1: Unlike the memoryless state feedback control law, the control input in (3) is a memory control strategy that depends on a new state that includes historical information in the SHW. Furthermore, the controller in the traditional direct sampling method loses all information between the adjacent sampling instants. Historical information is leveraged under the proposed SWI-based control strategy, which improves the control performance.

Remark 2: If N packets with SWIs are packed one to transmit over the network, the memory-based control law can be constructed as follows:

$$u(t) = \sum_{p=1}^{N} K_p \frac{\mu_p}{\bar{w}} \int_{t-w_p}^{t-w_{p-1}} x(s)ds \tag{4}$$

which improves the control performance. For simplicity, we assume that $K_i = K_j = K$ $(i, j = 1, \ldots, N)$. Thus, (4) degrades to (3).

Define $\varepsilon(t) = \bar{x}(i_k h) - \bar{x}(t_k h)$, where $i_k h = t_k h + \ell h$ is a sampling instant with $\ell = 0, 1, 2, \ldots, \bar{\ell}$ in $[t_k, t_{k+1})$.

By borrowing the idea of traditional ETMs, we develop the following new SWI-based ETM:

$$\psi(t) = \varepsilon^T(t)\Lambda\varepsilon(t) - \theta\bar{x}^T(i_k h)\Lambda\bar{x}(i_k h) \geq 0. \tag{5}$$

After the module of SWI-based ETM, we know that the next data-transmission event will be triggered at instant $t_{k+1}h$, which is determined by

$$t_{k+1}h = t_k h + \min_{\ell > 0}\{\ell h | \psi(t) \geq 0\}. \tag{6}$$

Remark 3: The use of historical information with forgetting factors as the input in the ETM in (5) can reduce the number of triggering events within a given time interval, in particular, when the system has uncertain random disturbances; only a few researches have studied this problem.

Remark 4: To apply reasonably historical information for the controller and ETM, μ_p is chosen such that it satisfies $\mu_1 > \mu_2 > \cdots > \mu_N$. Therefore, we call μ_p a forgetting factor; that is, the closer it is to the current time, the greater the weight of the state is. If we choose $\mu_i = \bar{w}/N$ $(i = 1, \ldots, N)$, it degenerates into the idea in [34].

Remark 5: In addition to the advantages presented in Remarks 1 and 3, the scheme for calculating the SWI and then implementing periodic sampling (Fig. 1) can prevent the Zeno phenomena.

Remark 6: If we set $N = 1$ and $\bar{w} \to 0$, (3) and (6) become the traditional state feedback control method and ETM, respectively.

Remark 7: As depicted in Fig. 1, the SWI is designed before the sampler. Hence, the control strategy becomes a memory control approach. This new control structure can be applied to the NCS and sampling control system, which have a wide range of applications, such as the control of oxygen and carbon dioxide contents in blood [35].

For $l = 0, 1, \ldots, \bar{l} - 1$, we define $\Omega_l \triangleq [t_k h + lh + d_l, t_k h + (l+1)h + d_{l+1})$ with $d_0 = \eta_k$ and $d_{\bar{l}} = \eta_{k+1}$, where η_k is a network-induced delay at instant $t_k h$. Thus, $\Omega \triangleq [t_k h + \eta_k, t_{k+1}h + \eta_{k+1}) = \cup_{l=0}^{\bar{l}-1}\Omega_l$.

Owing to the use of the ZOH, from (2), we have

$$\bar{x}(t) = \bar{x}(i_k h) = \sum_{p=1}^{N} \frac{\mu_p}{\bar{w}} \int_{t_k h + lh - w_p}^{t_k h + lh - w_{p-1}} x(s)ds \tag{7}$$

for $t \in \Omega_l$.

Defining $\eta(t) = t - (t_k h + lh)$ for $t \in \Omega_l$ results the following relationship:

$$\bar{x}(t) = \bar{x}(i_k h) = \sum_{p=1}^{N} \frac{\mu_p}{\bar{w}} \int_{t-\eta(t)-w_p}^{t-\eta(t)-w_{p-1}} x(s)ds. \tag{8}$$

According to the definition of $\eta(t)$ and Ω_l, one knows that $0 \leq \eta(t) \leq h + \bar{d}_l \triangleq \eta_M$.

We define a new time-varying variable $d_p(t) \triangleq \eta(t) + w_p$ for $t \in \Omega_l$, evidently, $p\bar{w} \leq d_p(t) \leq \eta_M + p\bar{w} \triangleq d_{pM}$. Thus, (8) can be converted into

$$\bar{x}(i_k h) = \frac{1}{\bar{w}} \sum_{p=1}^{N} \mu_p \int_{t-d_p(t)}^{t-\eta(t)-(p-1)\bar{w}} x(s)ds. \tag{9}$$

Thus, it is true that

$$\bar{x}(i_k h) = \frac{1}{\bar{w}} \sum_{p=1}^{N} \mu_p \Bigg[\int_{t-p\bar{w}}^{t-(p-1)\bar{w}} x(s)ds + \int_{t-d_p(t)}^{t-p\bar{w}} x(s)ds - \int_{t-d_{p-1}(t)}^{t-(p-1)\bar{w}} x(s)ds \Bigg]. \tag{10}$$

Before formulating the closed-loop system, we introduce the definition of Legendre polynomials

$$L_i(s) = (-1)^i \sum_{v=0}^{i} G_v^i \left(\frac{s-a}{b-a}\right)^i, \quad G_v^i = (-1)^i \binom{i}{v} \binom{i+v}{i} \tag{11}$$

and their properties.

1) For $\forall \nu \in \mathbb{N}$, $(b-a)\int_a^b \mathcal{L}_\nu^T(s)\mathcal{L}_\nu(s)ds = W_\nu$, where $\mathcal{L}_\nu(s) \triangleq [L_0(s) \cdots L_i(s) \cdots L_\nu(s)]^T$ and $W_\nu = \mathrm{diag}\{1, 3, \ldots, 2\nu + 1\}$.
2) $\dot{L}(s) = \begin{cases} 0, & i = 0 \\ \sum_{k=0}^{i-1} \frac{(2i+1)}{b-a}(1 - (-1)^{i+k}), & i \geq 1 \end{cases}$.
3) For $\forall i \in \mathbb{N}$, $L_i(a) = (-1)^i$, $L_i(b) = 1$.

Remark 8: In this study, we apply the above properties of Legendre polynomials to replace the method in which the approximate average measurement output in [34] is applied, thereby making the proof more solid, which has been a big challenge of this study.

By combining (1) and (10), we obtain the following closed-loop control system for $t \in \Omega_l$:

$$\dot{x}(t) = Ax(t) + BK \sum_{p=1}^{N} \frac{\mu_p}{\bar{w}} \int_{t-p\bar{w}}^{t-(p-1)\bar{w}} x(s)ds + BK \sum_{p=1}^{N} \frac{\mu_p}{\bar{w}} \int_{t-d_p(t)}^{t-p\bar{w}} x(s)ds$$

$$
\begin{aligned}
&- BK\sum_{p=1}^{N}\frac{\mu_p}{\bar{w}}\int_{t-d_{p-1}(t)}^{t-(p-1)\bar{w}} x(s)ds \\
&- BK\varepsilon(t) + Ed(t) \\
={}& Ax(t) - BK\varepsilon(t) + Ed(t) \\
&+ BK\sum_{p=1}^{N}\frac{\mu_p}{\bar{w}}\left[-\Omega_{1,1}^{p}(t) + \Omega_{2}^{p}(t) + \Omega_{3,1}^{p}(t)\right] \quad (12)
\end{aligned}
$$

where

$$
\begin{aligned}
\Omega_{1,1}^{p}(t) &= \int_{-d_{p-1}(t)}^{-(p-1)\bar{w}} \mathbb{L}^{1}(s)x(t+s)ds \\
\Omega_{2}^{p}(t) &= \int_{-p\bar{w}}^{-(p-1)\bar{w}} \mathbb{L}^{2}(s)x(t+s)ds \\
\Omega_{3,1}^{p}(t) &= \int_{-d_p(t)}^{-p\bar{w}} \mathbb{L}^{3}(s)x(t+s)ds.
\end{aligned}
$$

In this study, we develop a memory-based state feedback control strategy for system (1) with the proposed SWI-based ETM. The block diagram is depicted in Fig. 1.

III. Main Results

The following lemma is useful for the subsequent results.

Lemma 1: For matrices $R \in \mathbb{R}^{q\times q} > 0$, $Y \in \mathbb{R}^{q\times q}$, and $\mathcal{R} = \begin{bmatrix} R & Y \\ Y^T & R\end{bmatrix} > 0$ and the vector function $x : [a, b] \to \mathbb{R}^q$, we have

$$
\int_a^b \mathbf{Sy}(R, x(s))ds \geq \frac{1}{b-a}\mathbf{Sy}\left(\mathcal{R}\otimes W_\nu, \begin{bmatrix}\mathbb{K}_{q,\nu} & 0_{\nu q}\\ 0_{\nu q} & \mathbb{K}_{q,\nu}\end{bmatrix}\Omega_\nu\right) \quad (13)
$$

where $\Omega_\nu = \begin{bmatrix}\int_c^b \mathbb{L}_\nu(s)x(s)ds \\ \int_a^c \mathbb{L}_\nu(s)x(s)ds\end{bmatrix}$, $\mathbb{L}_\nu(s) \triangleq \mathcal{L}_\nu(s)\otimes I_q$, $c \in [a,\ b]$, and $W_\nu = \mathrm{diag}\{1, 3, \ldots, 2\nu+1\}$.

Proof: Let $\mathbf{f}(s) = \mathcal{L}_\nu(s)$ and $\varpi(s) = 1$ for [4, Lemma 3]; The proof is complete. ■

Remark 9: In (13), the matrix $\mathbb{K}_{q,\nu} \in \mathbb{R}^{q\nu\times q\nu}$ can be obtained by using the MATLAB instruction **vecperm**(q, ν) presented in [36]. It has the same property as that in [4, Lemma 2].

Theorem 1: For the scalars $\bar{w}$, α, θ, controller gain K, and prespecified H_∞ attenuation level γ, the system (12) is asymptotically stable if there exist symmetric matrices P, $R_{1p} > 0$, $R_{2p} > 0$, $R_{3p} > 0$, $Q_{1p} > 0$, $Q_{2p} > 0$, $Q_{3p} > 0$, $\Lambda > 0$, $\mathcal{Q}_{1(p-1)} > 0$, and $\mathcal{Q}_{3p} > 0$ with $p = 1, \ldots, N$, and a matrix G such that

$$
\mathscr{P} > 0 \quad \text{and} \quad \Theta < 0 \quad (14)
$$

where

$$
\begin{aligned}
\mathscr{P} &= P + \mathrm{diag}\{0, \mathfrak{Q}_1, \mathfrak{Q}_2, \mathfrak{Q}_3\} \\
\Theta &= \mathbf{He}(\mathcal{M}^T P\mathcal{H}) \\
&\quad + \sum_{p=1}^{N}\left[\mathbf{Sy}\left(\hat{\mathcal{T}}_{2p}, \mathbb{I}_{1+p}\right) - \mathbf{Sy}\left(R_{1p}, \mathbb{I}_{2+p+N}\right)\right] \\
&\quad - \mathbf{Sy}\left(W_\nu\otimes\mathfrak{Q}_1, \mathbf{K}\mathbb{I}_{1,N}\right) \\
&\quad + \sum_{p=1}^{N}\left[\mathbf{Sy}\left(\hat{\mathcal{T}}_{3p}, \mathbb{I}_{1+p}\right) - \mathbf{Sy}\left(R_{2p}, \mathbb{I}_{2+p}\right)\right] \\
&\quad + \sum_{p=1}^{N}\left[\mathbf{Sy}\left(\hat{\mathcal{T}}_{4p}, \mathbb{I}_{2+p}\right) - \mathbf{Sy}\left(R_{3p}, \mathbb{I}_{3+p+N}\right)\right] \\
&\quad - \mathbf{Sy}\left(W_\nu\otimes\mathfrak{Q}_2, \mathbb{I}_{2,N}\right) - \mathbf{Sy}\left(W_\nu\otimes\mathfrak{Q}_3, \mathbf{K}\mathbb{I}_{3,N}\right) \\
&\quad + \mathbf{Sy}\left(\begin{bmatrix}-\Lambda & 0\\ 0 & \theta\Lambda\end{bmatrix}, \begin{bmatrix}\mathbb{I}_\varepsilon \\ \mathbb{I}_{\bar{x}}\end{bmatrix}\right) - \gamma^2\mathbf{Sy}\left(I_q, \mathbb{I}_d\right) \\
&\quad - \mathbf{Sy}(I_r, \mathbb{I}_z) + \mathbf{He}\left(\mathbb{I}_z^T C\mathbb{I}_2\right) + \mathbf{He}(\mathcal{G}\mathcal{F}) \\
\mathfrak{Q}_1 &= \mathrm{diag}\left\{\frac{1}{\eta_M}\mathcal{Q}_{10}, \ldots, \frac{1}{\eta_M}\mathcal{Q}_{1p}, \ldots, \frac{1}{\eta_M}\mathcal{Q}_{1(N-1)}\right\} \\
\mathfrak{Q}_2 &= \mathrm{diag}\left\{\frac{1}{\bar{w}}\mathcal{Q}_{21}, \ldots, \frac{1}{\bar{w}}\mathcal{Q}_{2p}, \ldots, \frac{1}{\bar{w}}\mathcal{Q}_{2N}\right\} \\
\mathfrak{Q}_3 &= \mathrm{diag}\left\{\frac{1}{\eta_M}\mathcal{Q}_{31}, \ldots, \frac{1}{\eta_M}\mathcal{Q}_{3p}, \ldots, \frac{1}{\eta_M}\mathcal{Q}_{3N}\right\} \\
\mathcal{Q}_{1(p-1)} &= \begin{bmatrix}Q_{1p} & *\\ Y_{1p} & Q_{1p}\end{bmatrix},\ \mathcal{Q}_{2p} = Q_{2p},\ \mathcal{Q}_{3p} = \begin{bmatrix}Q_{3p} & *\\ Y_{3p} & Q_{3p}\end{bmatrix} \\
\mathbf{K} &= \mathrm{diag}\{\mathbb{K}, \ldots, \mathbb{K}\},\ \mathbb{K} = \begin{bmatrix}\mathbb{K}_{n,\nu+1} & 0_{(\nu+1)n}\\ 0_{(\nu+1)n} & \mathbb{K}_{n,\nu+1}\end{bmatrix} \\
\mathbb{I}_{\bar{x}} &= \sum_{p=1}^{N}\frac{\mu_p}{\bar{w}}\left[\mathbb{I}_{3+2N+2N(\nu+1)+p} - \mathbb{I}_{m(p,\nu,1,1)} + \mathbb{I}_{m(p,\nu,3,1)}\right] \\
m(p,\nu,j,k) &= 3 + 2N + 1.5(j-1)N(\nu+1) \\
&\quad + 2(p-1)(\nu+1) + k,\ j = 1, 3 \\
\hat{\mathcal{T}}_{2p} &= R_{1p} + \eta_M Q_{1p},\quad \mathbb{I}_\varepsilon = \mathbb{I}_{3+2N+5N(\nu+1)+1} \\
\hat{\mathcal{T}}_{3p} &= R_{2p} + \bar{w}Q_{2p},\quad \mathbb{I}_d = \mathbb{I}_{3+2N+5N(\nu+1)+2} \\
\hat{\mathcal{T}}_{4p} &= R_{3p} + \eta_M Q_{3p},\quad \mathbb{I}_z = \mathbb{I}_{3+2N+5N(\nu+1)+3} \\
\mathcal{F} &= -\mathbb{I}_1 + A\mathbb{I}_2 - BK\mathbb{I}_\varepsilon + E\mathbb{I}_d \\
&\quad + BK\sum_{p=1}^{N}\frac{\mu_p}{\bar{w}}\left[\mathbb{I}_2^p + \mathbb{I}_{3,1}^p - \mathbb{I}_{1,1}^p\right] \\
\mathbb{I}_{1,1}^p &= \mathbb{I}_{m(p,\nu,1,1)},\ \mathbb{I}_2^p = \mathbb{I}_{p+1},\ \mathbb{I}_{3,1}^p = \mathbb{I}_{m(p,\nu,3,1)} \\
\mathcal{G} &= \mathbb{I}_1^T G + \alpha\mathbb{I}_2^T G \\
\mathcal{M}^T &= \left[\mathbb{I}_2^T,\ \mathbb{I}_{1,N}^T,\ \mathbb{I}_{2,N}^T\ \mathbb{I}_{3,N}^T\right] \\
\mathcal{H}^T &= \left[\mathbb{I}_1^T,\ \mathbb{J}_{1,N}^T,\ \mathbb{J}_{2,N}^T,\ \mathbb{J}_{3,N}^T\right] \\
\mathbf{J}^T &= [I_n, \ldots, I_n],\ \hat{\mathbf{J}}^T = \left[(-1)^0 I_n, \ldots, (-1)^\nu I_n\right] \\
\mathbb{J}_{j,N}^T &= \left[{J_{j,N}^1}^T\ \ldots {J_{j,N}^p}^T,\ \ldots\ {J_{j,N}^N}^T\right],\ j = 1, 3 \\
J_{j,N}^p &= \mathbf{J}\mathbb{I}_{0.5(j+1)+p} - \hat{\mathbf{J}}\mathbb{I}_{0.5(j+3)+N+p} - \frac{\Pi_\nu}{\eta_M}\mathbb{I}_{1,N}^p \\
\mathbb{J}_{2,N} &= \begin{bmatrix}\mathbf{J}\mathbb{I}_{1+1} - \hat{\mathbf{J}}\mathbb{I}_{2+1} - \frac{\Pi_\nu}{\bar{w}}\mathbb{I}_{2,N}^1 \\ \vdots \\ \mathbf{J}\mathbb{I}_{1+p} - \hat{\mathbf{J}}\mathbb{I}_{2+p} - \frac{\Pi_\nu}{\bar{w}}\mathbb{I}_{2,N}^p \\ \vdots \\ \mathbf{J}\mathbb{I}_{1+N} - \hat{\mathbf{J}}\mathbb{I}_{2+N} - \frac{\Pi_\nu}{\bar{w}}\mathbb{I}_{2,N}^N\end{bmatrix} \\
{\mathbb{I}_{1,N}}^T &= \left[{\mathbb{I}_{1,N}^1}^T \cdots {\mathbb{I}_{1,N}^N}^T\right],\ {\mathbb{I}_{3,N}}^T = \left[{\mathbb{I}_{3,N}^1}^T \cdots {\mathbb{I}_{3,N}^N}^T\right] \\
\mathbb{I}_{2,N} &= \mathbb{E}_{2,N},\ \mathbb{I}_{1,N}^p = \mathbb{E}_{1,N}^{p,1} + \mathbb{E}_{1,N}^{p,2},\ \mathbb{I}_{2,N}^p = \mathbb{E}_{2,N}^p \\
\mathbb{I}_{3,N}^p &= \mathbb{E}_{3,N}^{p,1} + \mathbb{E}_{3,N}^{p,2},\ \mathbb{E}_{1,N}^T = \left[{\mathbb{E}_{1,N}^1}^T, \cdots {\mathbb{E}_{1,N}^N}^T\right] \\
\mathbb{E}_{2,N}^T &= \left[{\mathbb{E}_{2,N}^1}^T, \ldots, {\mathbb{E}_{2,N}^N}^T\right], \mathbb{E}_{3,N}^T = \left[{\mathbb{E}_{3,N}^1}^T \cdots {\mathbb{E}_{3,N}^N}^T\right]
\end{aligned}
$$

$$\mathbb{E}^{p}_{1,N}{}^{T} = \begin{bmatrix}\mathbb{E}^{p,1}_{1,N}{}^{T} & \mathbb{E}^{p,2}_{1,N}{}^{T}\end{bmatrix},\ \mathbb{E}^{p}_{3,N}{}^{T} = \begin{bmatrix}\mathbb{E}^{p,1}_{3,N}{}^{T} & \mathbb{E}^{p,2}_{3,N}{}^{T}\end{bmatrix}$$

$$\mathbb{E}^{p,1}_{j,N} = \begin{bmatrix}\mathbb{I}_{m(p,\nu,j,1)} \\ \vdots \\ \mathbb{I}_{m(p,\nu,j,(\nu+1))}\end{bmatrix},\ \mathbb{E}^{p,2}_{j,N} = \begin{bmatrix}\mathbb{I}_{m(p,\nu,j,(\nu+2))} \\ \vdots \\ \mathbb{I}_{m(p,\nu,j,2(\nu+1))}\end{bmatrix}$$

$$\mathbb{E}^{p}_{2,N} = \begin{bmatrix}\mathbb{I}_{3+2N+2N(\nu+1)+(p-1)(\nu+1)+1} \\ \vdots \\ \mathbb{I}_{3+2N+2N(\nu+1)+p(\nu+1)}\end{bmatrix}$$

$$\Pi_\nu = \begin{bmatrix}\pi^0_0 I & \cdots & \pi^\nu_0 I \\ \vdots & \pi^i_g & \vdots \\ \pi^0_\nu I & \cdots & \pi^\nu_\nu I\end{bmatrix}$$

$$\pi^i_g = \begin{cases}-(2i+1)\left(1-(-1)^{g+i}\right), & i \le g \\ 0, & i > g.\end{cases}$$

Proof: For simplicity, we define

$$\zeta(t) = \left[x^T(t), \mathscr{L}^{1T}(t), \mathscr{L}^{2T}(t), \mathscr{L}^{3T}(t)\ \right]^T$$

with $\mathscr{L}^1(t) = [\int_{-d_{0M}}^{0} \pounds_1^T(s,t)dv,\ \ldots \int_{-d_{(p-1)M}}^{-(p-1)\bar{w}} \mathscr{L}_1^T(s,t)ds$ $,\ldots, \int_{-d_{(N-1)M}}^{-(N-1)\bar{w}} \mathscr{L}_1^T(s,t)ds]^T$, $\mathscr{L}^2(t) = [\Omega_2^{1T}(t),\ldots,$ $\Omega_2^{pT}(t),\ldots,\ \Omega_2^{NT}(t)]$, $\mathscr{L}^3(t) = [\int_{-d_{1M}}^{-\bar{w}} \mathscr{L}_3^T(s,t)ds,\ldots,$ $\int_{-d_{pM}}^{-p\bar{w}} \mathscr{L}_3^T(s,t)ds,\ldots,\ \int_{-d_{NM}}^{-N\bar{w}} \mathscr{L}_3^T(s,t)ds]^T$, $\mathscr{L}_i(s,t) =$ $\mathbb{L}^i(s)x(t+s)$.

Construct the following Lyapunov function:

$$V(t) = V_1(t) + V_2(t) + V_3(t) + V_4(t) \tag{15}$$

where

$$\begin{aligned}
V_1(t) &= \zeta^T(t)P\zeta(t) \\
V_2(t) &= \sum_{p=1}^{N}\int_{-d_{(p-1)M}}^{-(p-1)\bar{w}} x^T(t+s)\left[\mathcal{T}_{2p} + sQ_{1p}\right]x(t+s)ds \\
V_3(t) &= \sum_{p=1}^{N}\int_{-p\bar{w}}^{-(p-1)\bar{w}} x^T(t+s)\left[\mathcal{T}_{3p} + sQ_{2p}\right]x(t+s)ds \\
V_4(t) &= \sum_{p=1}^{N}\int_{-d_{pM}}^{-p\bar{w}} x^T(t+s\left[\mathcal{T}_{4p} + sQ_{3p}\right]x(t+s)ds
\end{aligned}$$

with $\mathcal{T}_{2p} = R_{1p} + d_{(p-1)M}Q_{1p}$, $\mathcal{T}_{3p} = R_{2p} + p\bar{w}Q_{2p}$, and $\mathcal{T}_{4p} = R_{3p} + d_{pM}Q_{3p}$.

Taking the derivative of $V(t)$ along (12) results in

$$\dot{V}(t) = 2\zeta^T(t)P\dot{\zeta}(t) + \sum_{s=2}^{4}\sum_{p=1}^{N}\dot{V}_{sp}(t) \tag{16}$$

where

$$\begin{aligned}
\dot{V}_{2p}(t) &= x^T(t-(p-1)\bar{w})\hat{\mathcal{T}}_{2p}x(t-(p-1)\bar{w}) \\
&\quad - x^T\left(t-d_{(p-1)M}\right)R_{1p}x\left(t-d_{(p-1)M}\right) \\
&\quad - \int_{-d_{(p-1)M}}^{-(p-1)\bar{w}} x^T(t+s)Q_{1p}x(t+s)ds \\
\dot{V}_{3p}(t) &= x^T(t-(p-1)\bar{w})\hat{\mathcal{T}}_{3p}x(t-(p-1)\bar{w}) \\
&\quad - x^T(t-p\bar{w})R_{2p}x(t-p\bar{w}) \\
&\quad - \int_{-p\bar{w}}^{-(p-1)\bar{w}} x^T(t+s)Q_{2p}x(t+s)ds \\
\dot{V}_{4p}(t) &= x^T(t-p\bar{w})\hat{\mathcal{T}}_{4p}x(t-p\bar{w}) \\
&\quad - x^T\left(t-d_{pM}\right)R_{3p}x\left(t-d_{pM}\right) \\
&\quad - \int_{-d_{pM}}^{-p\bar{w}} x^T(t+s)Q_{3p}x(t+s)ds.
\end{aligned}$$

According to Lemma 1

$$\begin{aligned}
&-\sum_{p=1}^{N}\int_{-d_{(p-1)M}}^{-(p-1)\bar{w}} x^T(t+s)Q_{1(p-1)}x(t+s)ds \\
&\le [\mathbf{K}\Omega_1(t)]^T(W_\nu \otimes \mathfrak{Q}_1)[\mathbf{K}\Omega_1(t)] \\
&\quad - \sum_{p=1}^{N}\int_{-p\bar{w}}^{-(p-1)\bar{w}} x^T(t+s)Q_{2p}x(t+s)ds \\
&\le \left[\mathscr{L}^2(t)\right]^T(W_\nu \otimes \mathfrak{Q}_2)\left[\mathscr{L}^2(t)\right] \\
&\quad - \sum_{p=1}^{N}\int_{-d_{pM}}^{-p\bar{w}} x^T(t+s)Q_{3p}x(t+s)ds \\
&\le [\mathbf{K}\Omega_3(t)]^T(W_\nu \otimes \mathfrak{Q}_3)[\mathbf{K}\Omega_3(t)]
\end{aligned}$$

where

$$\begin{aligned}
\Omega_1(t) &= \begin{bmatrix}\Omega_1^{1^T}(t) & \cdots & \Omega_1^{p^T}(t) & \cdots & \Omega_1^{N^T}(t)\end{bmatrix}^T \\
\Omega_3(t) &= \begin{bmatrix}\Omega_3^{1^T}(t) & \cdots & \Omega_3^{p^T}(t) & \cdots & \Omega_3^{N^T}(t)\end{bmatrix}^T \\
\Omega_1^p(t) &= \begin{bmatrix}\Omega_{1,1}^p(t) \\ \Omega_{1,2}^p(t)\end{bmatrix},\ \Omega_3^p(t) = \begin{bmatrix}\Omega_{3,1}^p(t) \\ \Omega_{3,2}^p(t)\end{bmatrix} \\
\Omega_{1,2}^p(t) &= \int_{-d_{(p-1)M}}^{-d_{p-1}(t)} \mathbb{L}^1(s)x(t+s)ds \\
\Omega_{3,2}^p(t) &= \int_{-d_{pM}}^{-d_p(t)} \mathbb{L}^3(s)x(t+s)ds.
\end{aligned}$$

We recall the triggering condition in (6)

$$-\varepsilon^T(t)\Lambda\varepsilon(t) + \theta\bar{x}^T(i_kh)\Lambda\bar{x}(i_kh) \ge 0 \tag{17}$$

which is equivalent to

$$\begin{bmatrix}\varepsilon(t) \\ \bar{x}(i_kh)\end{bmatrix}^T\begin{bmatrix}-\Lambda & 0 \\ 0 & \theta\Lambda\end{bmatrix}\begin{bmatrix}\varepsilon(t) \\ \bar{x}(i_kh)\end{bmatrix} \ge 0. \tag{18}$$

According to the bound and differentiation property of $L_i(s)$

$$\begin{aligned}
\dot{\mathcal{L}}_1^p(t) &= \mathbf{J}x(t-(p-1)\bar{w}) - \hat{\mathbf{J}}x\left(t-d_{(p-1)M}\right) \\
&\quad - \frac{\Pi_\nu}{\eta_M}\left(\Omega_{1,1}^p(t) + \Omega_{1,2}^p(t)\right)
\end{aligned} \tag{19}$$

$$\dot{\mathcal{L}}_2^p(t) = \mathbf{J}x(t-(p-1)\bar{w}) - \hat{\mathbf{J}}x(t-p\bar{w}) - \frac{\Pi_\nu}{\bar{w}}\Omega_2^p(t) \tag{20}$$

$$\begin{aligned}
\dot{\mathcal{L}}_3^p(t) &= \mathbf{J}x(t-p\bar{w}) - \hat{\mathbf{J}}x\left(t-d_{pM}\right) \\
&\quad - \frac{\Pi_\nu}{\eta_M}\left(\Omega_{3,1}^p(t) + \Omega_{3,2}^p(t)\right).
\end{aligned} \tag{21}$$

By defining $\vartheta(t) = [\dot{x}^T(t), x^T(t), x^T(t-\bar{w}),\ldots,x^T(t-N\bar{w}), x^T(t-d_{0M}),\ldots,x^T(t-d_{NM}), \Omega_1^T(t), \Omega_2^T(t), \Omega_3^T(t)\varepsilon^T(t), d^T(t), z^T(t)]^T$, we obtain

$$\zeta(t) = \mathcal{M}\vartheta(t),\ \dot{\zeta}(t) = \mathcal{H}\vartheta(t). \tag{22}$$

From (12), one has

$$\vartheta^T(t)\mathbf{He}(\mathcal{G}\mathcal{F})\vartheta(t) = 0 \tag{23}$$

where $\mathcal{G} = \mathbb{I}_1^TG + \alpha\mathbb{I}_2^TG$.

To ensure H_∞ stability of system (12), the following condition is needed:

$$\begin{aligned}
&\dot{V}(t) + z^T(t)z(t) - \gamma^2 d^T(t)d(t) \le \vartheta^T(t)\mathbf{He}\big(\mathcal{M}^T P\mathcal{H}\big)\vartheta(t)\\
&\quad + \sum_{p=1}^{N}\Big[\mathbf{Sy}\Big(\hat{\mathcal{T}}_{2p}, \mathbb{I}_{1+p}\vartheta(t)\Big) - \mathbf{Sy}\big(R_{1p}, \mathbb{I}_{2+p+N}\vartheta(t)\big)\Big]\\
&\quad - \mathbf{Sy}\big(W_\nu \otimes \mathfrak{Q}_1, \mathbf{K}\mathbb{E}_{1,N}\vartheta(t)\big)\\
&\quad + \sum_{p=1}^{N}\Big[\mathbf{Sy}\Big(\hat{\mathcal{T}}_{3p}, \mathbb{I}_{1+p}\vartheta(t)\Big) - \mathbf{Sy}\big(R_{2p}, \mathbb{I}_{2+p}\vartheta(t)\big)\Big]\\
&\quad - \mathbf{Sy}\big(W_\nu \otimes \mathfrak{Q}_2, \mathbb{E}_{2,N}\vartheta(t)\big)\\
&\quad + \sum_{p=1}^{N}\Big[\mathbf{Sy}\Big(\hat{\mathcal{T}}_{4p}, \mathbb{I}_{2+p}\vartheta(t)\Big) - \mathbf{Sy}\big(R_{3p}, \mathbb{I}_{3+p+N}\vartheta(t)\big)\Big]\\
&\quad - \mathbf{Sy}\big(W_\nu \otimes \mathfrak{Q}_3, \mathbf{K}\mathbb{E}_{3,N}\vartheta(t)\big) - 0.2785\mu_0\\
&\quad + \mathbf{Sy}\left(\begin{bmatrix}-\Lambda & 0\\ 0 & \theta\Lambda\end{bmatrix}, \begin{bmatrix}\mathbb{I}_\varepsilon\\ \mathbb{I}_{\tilde{x}}\end{bmatrix}\vartheta(t)\right)\\
&\quad - \gamma^2\mathbf{Sy}\big(I_q, \mathbb{I}_d\vartheta(t)\big) - \mathbf{Sy}(I_r, \mathbb{I}_z\vartheta(t))\\
&\quad + \vartheta^T(t)\mathbf{He}\big(\mathbb{I}_z^T C\mathbb{I}_2\big)\vartheta(t) + \mathbf{Sy}(\mathbf{He}(\mathcal{G}\mathcal{F}), \vartheta(t)) < 0
\end{aligned}$$

which is guaranteed by (14). Thus, the proof is completed. ■

Remark 10: In this study, we focus on designing an event-triggered control method with SWI. Moreover, $V_3(t)$ and $V_4(t)$ in (15) help introduce SWI by using the properties of Legendre polynomials. In addition, P in $V_1(t)$ does not need to be positive definite; thus, the results are less conservative.

Theorem 2: For the scalars $\bar{w}$, α, θ, and the prespecified H_∞ attenuation level γ, the system (1) with the controller in (3) and the SWI-based ETM in (6) is asymptotically stable if there exist symmetric matrices $\tilde{P}$, $\tilde{R}_{1p} > 0$, $\tilde{R}_{2p} > 0$, $\tilde{R}_{3p} > 0$, $\tilde{Q}_{1p} > 0$, $\tilde{Q}_{2p} > 0$, $\tilde{Q}_{3p} > 0$, $\tilde{Y}_{1p} > 0$, $\tilde{Y}_{3p} > 0$, $\tilde{\Lambda} > 0$, $\tilde{\mathfrak{Q}}_{1(p-1)} = \begin{bmatrix}\tilde{Q}_{1p} & \tilde{Y}_{1p}\\ \tilde{Y}_{1p} & \tilde{Q}_{1p}\end{bmatrix} > 0$, and $\tilde{\mathfrak{Q}}_{3p} = \begin{bmatrix}\tilde{Q}_{3p} & \tilde{Y}_{3p}\\ \tilde{Y}_{3p} & \tilde{Q}_{3p}\end{bmatrix} > 0$ with $p = 1, \ldots, N$ and matrices X and Y such that

$$\tilde{\mathscr{P}} > 0, \text{ and } \tilde{\Theta} < 0 \tag{24}$$

where

$$\begin{aligned}
\tilde{\mathscr{P}} &= \tilde{P} + \mathrm{diag}\Big\{0, \tilde{\mathfrak{Q}}_1, \tilde{\mathfrak{Q}}_2, \tilde{\mathfrak{Q}}_3\Big\}\\
\tilde{\Theta} &= \mathbf{He}\big(\mathcal{M}^T\tilde{P}\mathcal{H}\big)\\
&\quad + \sum_{p=1}^{N}\Big[\mathbf{Sy}\Big(\tilde{\mathcal{T}}_{2p}, \mathbb{I}_{1+p}\Big) - \mathbf{Sy}\big(\tilde{R}_{1p}, \mathbb{I}_{2+p+N}\big)\Big]\\
&\quad - \mathbf{Sy}\Big(W_\nu \otimes \tilde{\mathfrak{Q}}_1, \mathbf{K}\mathbb{I}_{1,N}\Big)\\
&\quad + \sum_{p=1}^{N}\Big[\mathbf{Sy}\Big(\tilde{\mathcal{T}}_{3p}, \mathbb{I}_{1+p}\Big) - \mathbf{Sy}\big(\tilde{R}_{2p}, \mathbb{I}_{2+p}\big)\Big]\\
&\quad + \sum_{p=1}^{N}\Big[\mathbf{Sy}\Big(\tilde{\mathcal{T}}_{4p}, \mathbb{I}_{2+p}\Big) - \mathbf{Sy}\big(\tilde{R}_{3p}, \mathbb{I}_{3+p+N}\big)\Big]\\
&\quad - \mathbf{Sy}\Big(W_\nu \otimes \tilde{\mathfrak{Q}}_2, \mathbb{I}_{2,N}\Big) - \mathbf{Sy}\Big(W_\nu \otimes \tilde{\mathfrak{Q}}_3, \mathbf{K}\mathbb{I}_{3,N}\Big)\\
&\quad + \mathbf{Sy}\left(\begin{bmatrix}-\tilde{\Lambda} & 0\\ 0 & \theta\tilde{\Lambda}\end{bmatrix}, \begin{bmatrix}\mathbb{I}_\varepsilon\\ \mathbb{I}_{\tilde{x}}\end{bmatrix}\right) - \gamma^2\mathbf{Sy}\big(I_q, \mathbb{I}_d\big) - \mathbf{Sy}\big(I_r, \mathbb{I}_z\big)\\
&\quad + \mathbf{He}\big(\mathbb{I}_z^T CX\mathbb{I}_2\big) + \mathbf{He}\Big(\tilde{\mathcal{G}}\tilde{\mathcal{F}}\Big)\\
\tilde{\mathcal{G}} &= \mathbb{I}_1^T + \alpha\mathbb{I}_2^T\\
\tilde{\mathcal{F}} &= -X\mathbb{I}_1 + AX\mathbb{I}_2 + BY\mathbb{I}_{\tilde{x}} - BY\mathbb{I}_\varepsilon + E\mathbb{I}_d\\
&\quad + BY\sum_{p=1}^{N}\frac{\mu_p}{\bar{w}}\Big[\mathbb{I}_2^p + \mathbb{I}_{3,1}^p - \mathbb{I}_{1,1}^p\Big].
\end{aligned}$$

Then, the weight matrix of the SWI-based ETM and the controller gain can be solved with $\Lambda = X^{-1}\tilde{\Lambda}X^{-1}$ and $K = YX^{-1}$, respectively.

Proof: Define

$$\begin{aligned}
&X = G^{-1}, \ \tilde{P} = \big(I_{(1+5(\varrho+1))n} \otimes X\big)P\big(I_{(1+5(\varrho+1))n} \otimes X\big)\\
&\tilde{\mathcal{T}}_{sp} = X\hat{\mathcal{T}}_{sp}X, \quad \tilde{R}_{(s-1)p} = XR_{(s-1)p}X\\
&p = 1, 2, \ldots, N, \quad s = 2, 3, 4\\
&\tilde{\mathfrak{Q}}_1 = \mathcal{X}\mathfrak{Q}_1\mathcal{X}, \tilde{\mathfrak{Q}}_2 = \mathcal{X}_2\mathfrak{Q}_2\mathcal{X}_2, \tilde{\mathfrak{Q}}_3 = \mathcal{X}\mathfrak{Q}_3\mathcal{X}\\
&\mathcal{X} = I_{(N(\varrho+1))2n} \otimes X, \mathcal{X}_2 = I_{(N(\varrho+1))n} \otimes X\\
&\tilde{Y}_{1p} = XY_{1p}X, \quad \tilde{Y}_{3p} = XY_{3p}X, \quad \tilde{\Lambda} = X\Lambda X.
\end{aligned}$$

Pre- and post-multiplying (25) by $\mathscr{X} = \mathrm{diag}\{X, X, X_1, X_2, X, X, I, I\}$, $X_1 = \mathrm{diag}\{\underbrace{X, \ldots, X}_{2N}\}$, $X_2 = \mathrm{diag}\{\underbrace{X, \ldots, X}_{5N(\nu+1)}\}$ and its transpose yields

$$\tilde{\Theta} < 0 \tag{25}$$

which is ensured by (24). Thus, the proof is complete. ■

IV. Numerical Example

This section presents a simulation example to validate the proposed SWI-based event-triggered control strategy.

Example 1: Consider the system (1) with the following parameters:

$$A = \begin{bmatrix}0 & 1\\ 0.5 & -3\end{bmatrix}, \ B = \begin{bmatrix}0\\ 2\end{bmatrix}, \ E = \begin{bmatrix}5\\ 2\end{bmatrix}, \ C = \begin{bmatrix}2 & 1.5\end{bmatrix}.$$

Let the sampling period be $h = 0.005$ s and the possible maximum transmission delay be $\bar{d}_l = 0.05$ s, then $\eta_M = \bar{d}_l + h = 0.055$ s.

The scale of the SHW is $w = 0.045$ s. Three parts ($N = 3$) with the weights $\mu_1 = 0.6$, $\mu_2 = 0.3$, and $\mu_3 = 0.1$ are segmented. For $\gamma = 1$, $\theta = 0.05$, and $\alpha = 150$, we obtain the controller gain in (3) and the triggering parameter of the ETM in (5) from Theorem 2 with the MATLAB Toolbox:

$$K = \begin{bmatrix}-1.0309 & -0.6962\end{bmatrix}, \ \Lambda = \begin{bmatrix}0.3428 & 0.2315\\ 0.2315 & 0.1564\end{bmatrix}. \tag{26}$$

The initial condition is $x(0) = [2 \ -1]^T$; and the disturbance is $d(t) = r(t)e^{-0.5t}$ for $0 < t < 6$ s and zero for $t > 6$ s, where $r(t)$ denotes a stochastic variable satisfying $|r(t)| < 10$.

For the previously presented parameters, we obtain the simulation results shown in Fig. 2; evidently, the system can successfully be stabilized under the proposed communication and control scheme.

To show the influence of the segmented weight on the system performance and the amount of transmitted data, we set $N = 1$; that is, the state in the whole SHW has the weight $\mu = 1$. The other parameters are identical to those for the

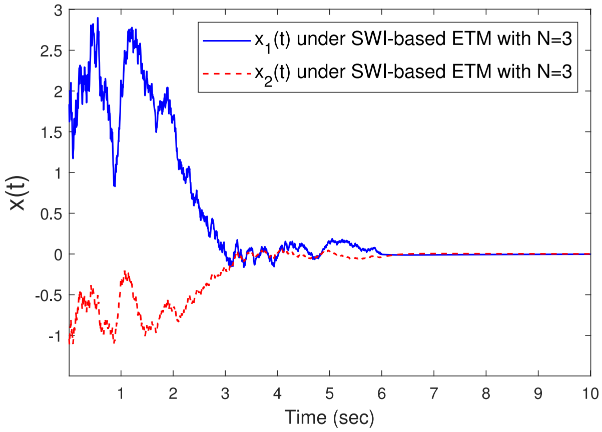

Fig. 2. State responses under the SWI-based ETM with $N = 3$.

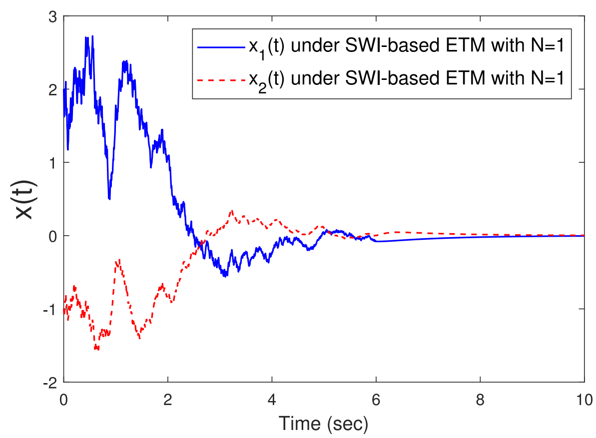

Fig. 3. State responses under SWI-based ETM with $N = 1$.

case with $N = 3$. Similarly, we obtain the parameters of the controller in (3) and the SWI-based ETM in (5) via Theorem 2

$$K = \begin{bmatrix} -2.1088 & -1.5404 \end{bmatrix}, \quad \Lambda = \begin{bmatrix} 2.6819 & 1.9590 \\ 1.9590 & 1.4311 \end{bmatrix}. \quad (27)$$

Fig. 3 presents the state responses for these parameters. According to Figs. 2 and 3, one can know that the control strategy and ETM with SWI, where $N = 1$ and $N = 3$, can result in good control performance.

To investigate the amount of transmitted data under the traditional ETM, the SWI-based ETM with ($N = 1$), and our proposed SWI-based ETM ($N = 3$), the release instants and their corresponding release intervals are presented in Fig. 4. Evidently, our proposed SWI-based ETM leads to fewer transmitted data. Table I presents the detailed amount of transmitted data; only 14.2% of the sampling packets are transmitted over the network if the proposed SWI-based ETM with $N = 3$ is adopted, 16.5% is transmitted for $N = 1$; by contrast, the data-release rate increases to 20.3% for traditional ETM. Therefore, our proposed SWI-based ETM can significantly save network communication resources while maintaining the control performance at a certain level.

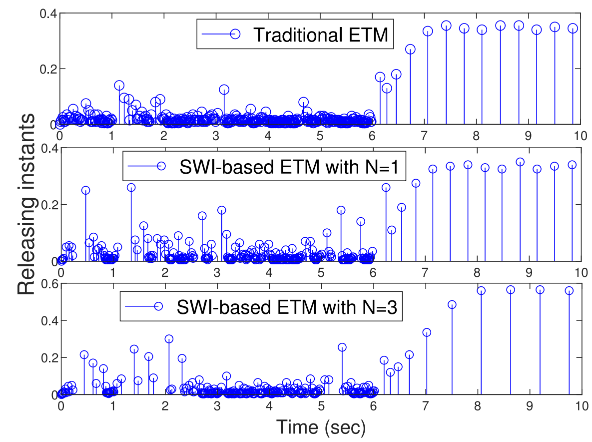

Fig. 4. Releasing instants under the traditional ETM in [24] and SWI-based ETMs with $N = 1$ and 3.

TABLE I
AMOUNT OF DATA TRANSMISSION ($\mathcal{N}$) UNDER DIFFERENT COMMUNICATION MECHANISMS

Communication mechanism	$\mathcal{N}$
Traditional ETM in [24]	406
SWI-based ETM with $N = 1$	330
SWI-based ETM with $N = 3$	284

TABLE II
AMOUNT OF TRANSMITTED DATA ($\mathcal{N}$) OF DIFFERENT COMMUNICATION MECHANISMS

Communication mechanism	$\mathcal{N}$
Traditional ETM in [24]	560
SWI-based ETM with $N = 1$	493
SWI-based ETM with $N = 3$	388

Example 2: In this example, we consider the decoupled linearized dynamics of a practical F-18 aircraft studied in [37]

$$\begin{bmatrix} \dot{\alpha}(t) \\ \dot{q}(t) \end{bmatrix} = \begin{bmatrix} -1.175 & 0.9871 \\ -8.45 & -0.8776 \end{bmatrix} \begin{bmatrix} \alpha(t) \\ q(t) \end{bmatrix} + \begin{bmatrix} -0.194 & -0.03593 \\ -19.29 & -3.803 \end{bmatrix} \begin{bmatrix} \delta_E(t) \\ \delta_{PTV}(t) \end{bmatrix} + \begin{bmatrix} 1 \\ 4 \end{bmatrix} d(t)$$

where $\alpha(t)$ and $q(t)$ are the attack angle and pitch rate; they are chosen as the state. The control inputs are the symmetric elevator position $\delta_E(t)$ and symmetric pitch thrust velocity nozzle position $\delta_{\text{PTV}}(t)$.

For $\gamma = 1$, by solving the conditions in Theorem 2 with the design parameters in Example 1, we obtain the controller gains and triggering matrices for $N = 1$ and $N = 3$

$$K = \begin{bmatrix} 89.9648 & 56.0419 \\ -456.3525 & -284.1305 \end{bmatrix}, \quad \Lambda = \begin{bmatrix} 0.2541 & 0.2262 \\ 0.2262 & 0.3030 \end{bmatrix}$$

for $N = 1$ and

$$K = \begin{bmatrix} 33.1511 & -1.5255 \\ -168.1628 & 7.8409 \end{bmatrix}, \quad \Lambda = \begin{bmatrix} 0.0654 & -0.0021 \\ -0.0021 & 0.0530 \end{bmatrix},$$

for $N = 3$.

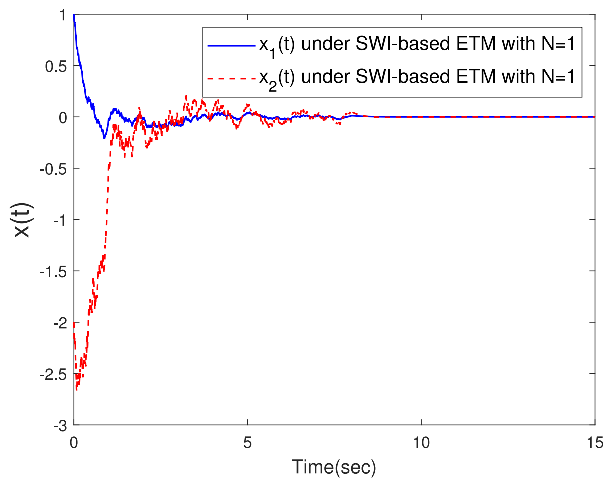

Fig. 5. State responses of the F-18 aircraft under the SWI-based ETM with $N = 1$.

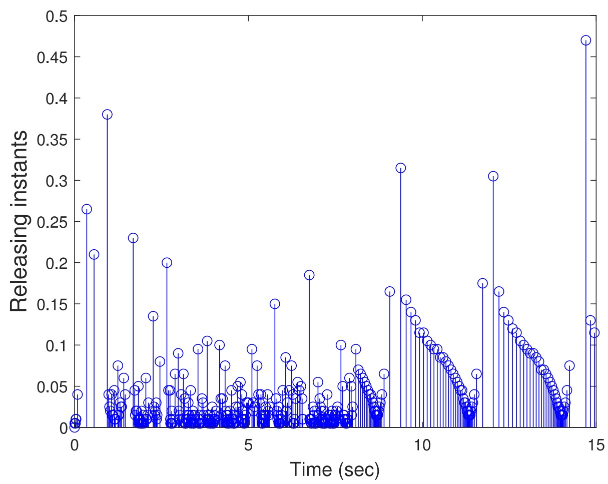

Fig. 6. Release instants and release intervals under SWI-based ETM with $N = 1$.

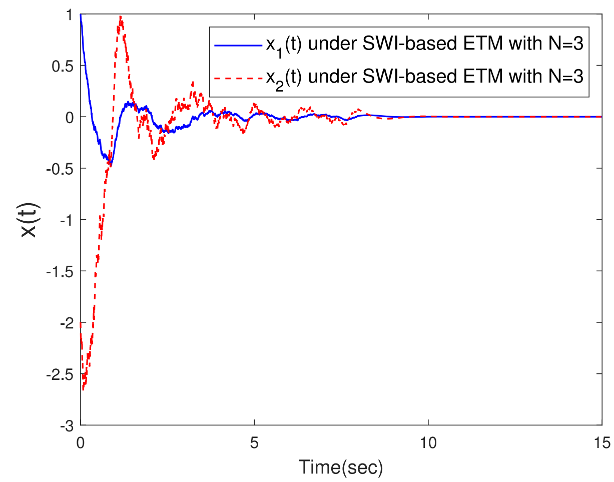

Fig. 7. State responses of the F-18 aircraft under the SWI-based ETM with $N = 3$.

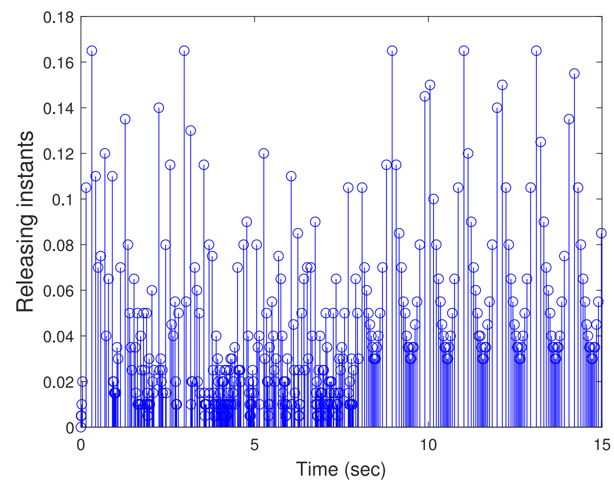

Fig. 8. Release instants and release intervals under SWI-based ETM with $N = 3$.

The initial condition is assumed to be $x(0) = [1 \quad -2]^\top$, and the disturbance is $d(t) = r(t)e^{-0.3t}$ for $0 < t < 8$ s, and 0 for $t > 8$ s, where $r(t)$ is a stochastic variable satisfying $|r(t)| < 5$.

The state responses and triggering instants for $N = 1$ and $N = 3$ are presented in Figs. 5–8. Moreover, the amount of transmitted data under the traditional ETM, SWI-based ETM for $N = 1$, and proposed SWI-based ETM for $N = 3$ are presented in Table II. From these figures and the table, we can get similar conclusions from Example 1 that the proposed SWI-based ETM helps reduce redundant triggering events and saves more network resources, in particular for systems subject to random disturbances.

V. Conclusion

An SWI-based event-triggered control method forNCSs was developed. The sampler samples SWI in the SWH from the plant rather than the current state or current measurement output. This processing method can reduce the loss of information caused by direct periodic sampling. Furthermore, using the historical averaged information as the decision variable instead of the information of certain instants is more reasonable, in particular, for a system with uncertain or stochastic disturbances. In addition, the Zeno phenomenon is prevented. The simulation example shows that this proposed method fully exploit historical information and effectively balance the system performance and use of network resources. In the future, the proposed SWI-based ETM can be extended to nonlinear systems by combining the methods in [38], [39], and [40] to address practical problems.

References

[1] X. Ge, Q.-L. Han, and X.-M. Zhang, “Achieving cluster formation of multi-agent systems under aperiodic sampling and communication delays,” *IEEE Trans. Ind. Electron.*, vol. 65, no. 4, pp. 3417–3426, Apr. 2018.

[2] L. X. Zhang, Z. P. Ning, and W. X. Zheng, “Observer-based control for piecewise-affine systems with both input and output quantization,” *IEEE Trans. Autom. Control*, vol. 62, no. 11, pp. 5858–5865, Nov. 2017.

[3] H.-B. Zeng, K. L. Teo, and Y. He, “A new looped-functional for stability analysis of sampled-data systems,” *Automatica*, vol. 82, pp. 328–331, Aug. 2017.

[4] B. Priya and S. Manohar, “Adaptive power control and duty cycle based medium access control protocol for cluster based wireless sensor network,” *Rom. J. Inf. Sci. Technol.*, vol. 23, no. 1, pp. 38–54, 2020.

[5] J. Lai, X. Lu, X. Yu, W. Yao, J. Wen, and S. Cheng, "Distributed multi-DER cooperative control for master-slave-organized microgrid networks with limited communication bandwidth," *IEEE Trans. Ind. Informat.*, vol. 15, no. 6, pp. 3443–3456, Jun. 2019.

[6] H. Yan, P. Li, H. Zhang, X. Zhan, and F. Yang, "Event-triggered distributed fusion estimation of networked multisensor systems with limited information," *IEEE Trans. Syst., Man, Cybern., Syst.*, vol. 50, no. 12, pp. 5330–5337, Dec. 2020.

[7] Z. Gu, P. Shi, D. Yue, and Z. Ding, "Decentralized adaptive event-triggered H_∞ filtering for a class of networked nonlinear interconnected systems," *IEEE Trans. Cybern.*, vol. 49, no. 5, pp. 1570–1579, May 2019.

[8] H. Zhang, J. Liu, and S. Xu, "H_∞ load frequency control of networked power systems via an event-triggered scheme," *IEEE Trans. Ind. Electron.*, vol. 67, no. 8, pp. 7104–7113, Aug. 2020.

[9] T. Tian and S. Sun, "Distributed fusion estimation for multisensor multirate systems with packet dropout compensations and correlated noises," *IEEE Trans. Syst., Man, Cybern., Syst.*, vol. 51, no. 9, pp. 5762–5772, Sep. 2021.

[10] H. Li, X. Li, and H. Zhang, "Optimal control for discrete-time NCSs with input delay and Markovian packet losses: Hold-input case," *Automatica*, vol. 132, Oct. 2021, Art. no. 109806.

[11] D. Yue, Q.-L. Han, and J. Lam, "Network-based robust H_∞ control of systems with uncertainty," *Automatica*, vol. 41, no. 6, pp. 999–1007, Jun. 2005.

[12] E. Fridman, "A refined input delay approach to sampled-data control," *Automatica*, vol. 46, no. 2, pp. 421–427, Feb. 2010.

[13] K. Liu and E. Fridman, "Wirtinger's inequality and Lyapunov-based sampled-data stabilization," *Automatica*, vol. 48, no. 1, pp. 102–108, Jan. 2012.

[14] L. Hetel, C. Fiter, H. Omran, A. Seuret, E. Fridman, J.-P. Richard, and S. I. Niculescu, "Recent developments on the stability of systems with aperiodic sampling: An overview," *Automatica*, vol. 76, pp. 309–335, Feb. 2017.

[15] J. Chen, S. Meng, and J. Sun, "Stability analysis of networked control systems with aperiodic sampling and time-varying delay," *IEEE Trans. Cybern.*, vol. 47, no. 8, pp. 2312–2320, Aug. 2017.

[16] F. Forni, S. Galeani, D. Nešić, and L. Zaccarian, "Event-triggered transmission for linear control over communication channels," *Automatica*, vol. 50, no. 2, pp. 490–498, Feb. 2014.

[17] W. Zhang and L. Yu, "BIBO stability and stabilization of networked control systems with short time-varying delays," *Int. J. Robust Nonlinear Control*, vol. 21, no. 3, pp. 295–308, Jan. 2011.

[18] A. Girard, "Dynamic triggering mechanisms for event-triggered control," *IEEE Trans. Autom. Control*, vol. 60, no. 7, pp. 1992–1997, Jul. 2015.

[19] X. Ge, Q.-L. Han, and Z. Wang, "A dynamic event-triggered transmission scheme for distributed set-membership estimation over wireless sensor networks," *IEEE Trans. Cybern.*, vol. 49, no. 1, pp. 171–183, Jan. 2019.

[20] D. Yue, E. Tian, and Q.-L. Han, "A delay system method for designing event-triggered controllers of networked control systems," *IEEE Trans. Autom. Control*, vol. 58, no. 2, pp. 475–481, Feb. 2013.

[21] Z. Lian, P. Shi, and C.-C. Lim, "Hybrid-triggered interval type-2 fuzzy control for networked systems under attacks," *Inf. Sci.*, vol. 567, pp. 332–347, Aug. 2021.

[22] X.-M. Zhang and Q.-L. Han, "Event-based H_∞ filtering for sampled-data systems," *Automatica*, vol. 51, pp. 55–69, Jan. 2015.

[23] Y. Wen, C. Jiao, X. Su, and P. Shi, "Event-triggered sliding-mode control of networked fuzzy systems with strict dissipativity," *IEEE Trans. Fuzzy Syst.*, vol. 30, no. 5, pp. 1371–1381, May 2022.

[24] S. Hu, D. Yue, X. Xie, X. Chen, and X. Yin, "Resilient event-triggered controller synthesis of networked control systems under periodic DoS jamming attacks," *IEEE Trans. Cybern.*, vol. 49, no. 12, pp. 4271–4281, Dec. 2019.

[25] Z. Gu, C. K. Ahn, D. Yue, and X. Xie, "Event-triggered H_∞ filtering for T–S Fuzzy-model-based nonlinear networked systems with multisensors against DoS attacks," *IEEE Trans. Cybern.*, vol. 52, no. 6, pp. 5311–5321, Jun. 2022, doi: 10.1109/TCYB.2020.3030028.

[26] W. Qi, Y. Hou, G. Zong, and C. K. Ahn, "Finite-time event-triggered control for semi-Markovian switching cyber-physical systems with FDI attacks and applications," *IEEE Trans. Circuits Syst. I, Reg. Papers*, vol. 68, no. 6, pp. 2665–2674, Jun. 2021.

[27] E. Tian and C. Peng, "Memory-based event-triggering H_∞ load frequency control for power systems under deception attacks," *IEEE Trans. Cybern.*, vol. 50, no. 11, pp. 4610–4618, Nov. 2020.

[28] Y. Shi, E. Tian, S. Shen, and X. Zhao, "Adaptive memory-event-triggered H_∞ control for network-based T–S fuzzy systems with asynchronous premise constraints," *IET Control Theory Appl.*, vol. 15, pp. 534–544, Mar. 2021.

[29] A. Selivanov and E. Fridman, "Event-triggered H_∞ control: A switching approach," *IEEE Trans. Autom. Control*, vol. 61, no. 10, pp. 3221–3226, Oct. 2016.

[30] S. Yan, Z. Gu, and C. K. Ahn, "Memory-event-triggered H_∞ filtering of unmanned surface vehicles with communication delays," *IEEE Trans. Circuits Syst. II, Exp. Briefs*, vol. 68, no. 7, pp. 2463–2467, Jul. 2021.

[31] J. Yang, Q. Zhong, K. Shi, and S. Zhong, "Dynamic-memory event-triggered H_∞ load frequency control for reconstructed switched model of power systems under hybrid attacks," *IEEE Trans. Cybern.*, early access, May 13, 2022, doi: 10.1109/TCYB.2022.3170560.

[32] H. Yu and F. Hao, "Input-to-state stability of integral-based event-triggered control for linear plants," *Automatica*, vol. 85, pp. 248–255, Nov. 2017.

[33] Q. Sun, J. Chen, and Y. Shi, "Integral-type event-triggered model predictive control of nonlinear systems with additive disturbance," *IEEE Trans. Cybern.*, vol. 51, no. 12, pp. 5921–5929, Dec. 2021.

[34] Z. Gu, C. K. Ahn, S. Yan, X. Xie, and D. Yue, "Event-triggered filter design based on average measurement output for networked unmanned surface vehicles," *IEEE Trans. Circuits Syst. II, Exp. Briefs*, vol. 69, no. 9, pp. 3804–3808, Sep. 2022, doi: 10.1109/TCSII.2022.3175221.

[35] G. Rigatos, P. Siano, D. Selisteanu, and R. E. Precup, "Nonlinear optimal control of oxygen and carbon dioxide levels in blood," *Intell. Ind. Syst.*, vol. 3, no. 2, pp. 61–75, Jun. 2017.

[36] N. J. Higham and M. Mikaitis, "Anymatrix: An extensible MATLAB matrix collection," *Numer. Algorithm.*, vol. 90, no. 3, pp. 1175–1196, Jul. 2022.

[37] G.-H. Yang and D. Ye, "Reliable H_∞ control of linear systems with adaptive mechanism," *IEEE Trans. Autom. Control*, vol. 55, no. 1, pp. 242–247, Jan. 2010.

[38] R. Precup, M. Tomescu, and S. Preitl, "Lorenz system stabilization using fuzzy controllers," *Int. J. Comput. Commun. Control*, vol. 2, no. 3, pp. 279–287, Sep. 2007.

[39] Y. Li, T. Wang, W. Liu, and S. Tong, "Neural network adaptive output-feedback optimal control for active suspension systems," *IEEE Trans. Syst., Man, Cybern., Syst.*, vol. 52, no. 6, pp. 4021–4032, Jun. 2022.

[40] R.-C. Roman et al., "Iterative feedback tuning algorithm for tower crane systems," *Procedia Comput. Sci.*, vol. 199, pp. 157–165, Feb. 2022.

Zhou Gu (Member, IEEE) received the B.S. degree in automation from North China Electric Power University, Beijing, China, in 1997, and the M.S. and Ph.D. degrees in control science and engineering from the Nanjing University of Aeronautics and Astronautics, Nanjing, China, in 2007 and 2010, respectively.

From September 1999 to January 2013, he was with the School of Power engineering, Nanjing Normal University, Nanjing, as an Associate Professor. He is currently a Professor with Nanjing Forestry University, Nanjing. His current research interests include networked control systems, time-delay systems, and reliable control and their applications.

Dong Yue (Fellow, IEEE) received the Ph.D. degree in engineering from the South China University of Technology, Guangzhou, China, in 1995.

He is currently a Professor and the Dean of the Institute of Advanced Technology for Carbon Neutrality, Nanjing University of Posts and Telecommunications, Nanjing, China, and also a Changjiang Professor with the Department of Control Science and Engineering, Huazhong University of Science and Technology, Wuhan, China. Up to now, he has published more than 100 papers in international journals. His research interests include analysis and synthesis of networked control systems, multiagent systems, optimal control of power systems, and Internet of Things.

Dr. Yue is currently an Associate Editor of the IEEE Control Systems Society Conference Editorial Board and also an Associate Editor of the IEEE TRANSACTIONS ON INDUSTRIAL INFORMATICS, *IEEE Industrial Electronics Magazine*, IEEE TRANSACTIONS ON SYSTEMS, MAN, AND CYBERNETICS, PART—A: SYSTEMS AND HUMANS, and IEEE TRANSACTIONS ON NEURAL NETWORKS AND LEARNING SYSTEMS from 2016 to 2018.

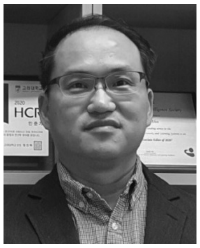

Choon Ki Ahn (Senior Member, IEEE) received the B.S. and M.S. degrees from the School of Electrical Engineering, Korea University, Seoul, South Korea, in 2000 and 2002, respectively, and the Ph.D. degree from the School of Electrical Engineering and Computer Science, Seoul National University, Seoul, 2006.

He is currently a Crimson Professor of Excellence with the College of Engineering and a Full Professor with the School of Electrical Engineering, Korea University.

Prof. Ahn was the recipient of the Early Career Research Award of Korea University in 2015. He is the recipient of the Highly Cited Researcher Award in Engineering by Clarivate Analytics (formerly, Thomson Reuters). In 2016, he was ranked #1 in Electrical/Electronic Engineering among Korean young professors based on research quality. In 2017, he received the Presidential Young Scientist Award from the President of South Korea. In 2020, he received the Outstanding Associate Editor Award for IEEE Transactions on Neural Networks and Learning Systems. In 2021, he received the Best Associate Editor Award for IEEE Transactions on Systems, Man, and Cybernetics: Systems. From 2019 to 2022, he received the Research Excellence Award from Korea University (Top 3% Professor of Korea University in Research). He has been a Senior Editor of IEEE Transactions on Neural Networks and Learning Systems, a Senior Associate Editor of IEEE Systems Journal, and an Associate Editor of IEEE Transactions on Fuzzy Systems, IEEE Transactions on Systems, Man, and Cybernetics: Systems, IEEE Transactions on Automation Science and Engineering, IEEE Transactions on Intelligent Transportation Systems, IEEE Transactions on Circuits and Systems—I: Regular Papers; *IEEE Systems, Man, and Cybernetics Magazine*, *Nonlinear Dynamics*, *Aerospace Science and Technology*, and other flagship journals.

Shen Yan received the B.S. and Ph.D. degrees from the College of Electrical Engineering and Control Science, Nanjing Technology University, Nanjing, China, in 2014 and 2019, respectively.

He is currently an Associate Professor with the College of Mechanical and Electronic Engineering, Nanjing Forestry University, Nanjing. His current research interests include networked control systems, nonlinear systems, and event-triggered control.

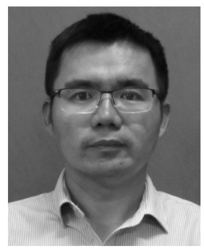

Xiangpeng Xie (Member, IEEE) received the B.S. and Ph.D. degrees in engineering from Northeastern University, Shenyang, China, in 2004 and 2010, respectively.

From 2012 to 2014, he was a Postdoctoral Fellow with the Department of Control Science and Engineering, Huazhong University of Science and Technology, Wuhan, China. He is currently a Professor with the Institute of Advanced Technology, Nanjing University of Posts and Telecommunications, Nanjing, China. His research interests include fuzzy modeling and control synthesis, state estimations, optimization in process industries, and intelligent optimization algorithms.